DALTON
FULL PAPER

Cationic manganese(I) tricarbonyl complexes with group 15 and 16 donor ligands: synthesis, multinuclear NMR spectroscopy and crystal structures

Julie Connolly, Anthony R. J. Genge, William Levason, Simon D. Orchard, Simon J. A. Pope and Gillian Reid

Department of Chemistry, University of Southampton, Highfield, Southampton, UK SO17 1BJ

Received 9th April 1999, Accepted 27th May 1999

The compound $[MnBr(CO)_5]$ reacted with [10]aneS$_3$ (1,4,7-trithiacyclodecane) in dmf solution to yield *fac*-$[Mn(CO)_3([10]aneS_3)]Br$. The compounds *fac*-$[Mn(CO)_3(L)]CF_3SO_3$ (L = $MeS(CH_2)_2S(CH_2)_2SMe$, $MeSe(CH_2)_3Se(CH_2)_3SeMe$, $MeC(CH_2SMe)_3$, $MeC(CH_2SeMe)_3$, $MeC(CH_2TeMe)_3$, $MeC(CH_2TePh)_3$, $MeC(CH_2PPh_2)_3$ $MeC(CH_2AsMe_2)_3$ or $Ph_2P(CH_2)_2PPh(CH_2)_2PPh_2$) were readily obtained by treatment of *fac*-$[Mn(CO)_3(Me_2CO)_3]CF_3SO_3$ with L at room temperature in Me_2CO solution. Similar reactions using three molar equivalents of PPh_2H, PCy_2H or $PPhH_2$ (L) yielded *fac*-$[Mn(CO)_3(L)_3]CF_3SO_3$ as pale yellow solids. The compounds have been characterised by analysis, IR and multinuclear NMR spectroscopy (^{1}H, ^{13}C-{^{1}H}, ^{31}P-{^{1}H}, ^{55}Mn, ^{77}Se-{^{1}H} and ^{125}Te-{^{1}H}), mass spectrometry and by single crystal X-ray diffraction studies on seven examples. The compounds all adopt a distorted octahedral arrangement with C_{3v} local symmetry at Mn^I, and three mutually *fac* carbonyl ligands. The δ(^{55}Mn) linewidths are very dependent upon subtle changes in the electric field gradient and for some of the phosphine complexes quartet coupling to ^{31}P is clearly resolved giving $^1J_{MnP}$ *ca.* 200 Hz. The spectroscopic data are discussed in terms of the relative bonding properties of the Group 15 or 16 donor ligands within the manganese(I) cation.

Introduction

It is widely accepted that thio-, seleno- and telluro-ethers are rather poorer ligands for transition metal centres compared to phosphines and arsines. Within the Group 16 ligands themselves the reduction in electronegativity down the group is expected to lead to improved σ-bonding capability, although experimental evidence to support this is sparse.[1] Some years ago Schumann *et al.*[2] conducted theoretical and experimental studies on the binding of Me_2E (E = S, Se or Te) which did support this prediction. These studies were based upon cyclopentadienyliron carbonyl species and similar studies were not undertaken on other metal centres. Complexes of manganese(I) carbonyls with varying degrees of substitution are extremely well known and a wide range of different ligand types can be introduced readily.[3] These species also offer a number of very good spectroscopic probes (IR (ν_{CO}), ^{1}H, ^{13}C-{^{1}H} and ^{55}Mn NMR) through which to examine subtle differences in bonding capabilities and are therefore ideal candidates for this type of study. Recently we have probed the relative donating abilities of the Group 16 donor atoms through detailed spectroscopic studies on *fac*-$[MX(CO)_3(E–E)]$ (M = Mn or Re; X = Cl, Br or I; E–E = dithio-, diseleno- or ditelluro-ether). Through this work we have shown that IR, ^{77}Se, ^{125}Te and ^{55}Mn NMR studies are all consistent with E→Mn σ donation increasing according to the series S < Se ≪ Te.[4] We have conducted similar studies on Group 15 ligand complexes.[5] In our final paper in this series we have extended our studies to cationic manganese(I) complexes involving Group 15 and 16 ligand types in order to investigate the trends more thoroughly. We report here the results of our studies on a range of cationic compounds involving the $Mn(CO)_3^+$ fragment and tridentate thio-, seleno-, telluro-ether, phosphine or arsine ligands, or monodentate primary or secondary phosphine ligands, including multinuclear NMR studies and a discussion of the trends observed. The rhenium(I) species *fac*-$[Re(CO)_3\{MeC(CH_2SeMe)_3\}]^+$ is also included. There are few examples of manganese(I) tricarbonyl complexes involving tridentate Group 15 and 16 donor ligands, and only one structurally characterised example, *fac*-$[Mn(CO)_3([9]aneS_3)]^+$,[6] hence we have also verified the structures of several of the compounds in this work, including *fac*-$[Mn(CO)_3(MeSCH_2CH_2SCH_2CH_2SMe)]CF_3SO_3$, *fac*-$[Mn(CO)_3([10]aneS_3)]_2[MnBr_4]$, *fac*-$[M(CO)_3\{MeC(CH_2EMe)_3\}]CF_3SO_3$ (M = Mn, E = S or Se; M = Re, E = Se), *fac*-$[Mn(CO)_3\{MeC(CH_2TePh)\}_3]CF_3SO_3$ and *fac*-$[Mn(CO)_3\{MeC(CH_2PPh_2)_3\}]CF_3SO_3$, through single crystal X-ray diffraction studies. A preliminary communication describing certain aspects of this work and the structure of *fac*-$[Mn(CO)_3\{MeC(CH_2TeMe)_3\}]CF_3SO_3$ has appeared.[7] The compound *fac*-$[Mn(CO)_3\{MeC(CH_2PPh_2)_3\}]^+$ has been prepared previously, albeit *via* a different route to the one which we use here,[8] while *fac*-$[Mn(CO)_3\{MeC(CH_2AsMe_2)_3\}]^+$ was reported in the mid-1960s.[9] In addition to the new compounds reported here, we have reprepared these compounds to provide a complete set of directly comparable spectroscopic data. The *mer* isomer of the dicarbonyl species $[MnX(CO)_2\{Ph_2P(CH_2)_2PPh(CH_2)_2PPh_2\}]$ is also known.[10]

Results and discussion

Reaction of $[MnBr(CO)_5]$ with [9]aneS$_3$ or [10]aneS$_3$ in dmf solution yields the complexes *fac*-$[Mn(CO)_3([9]aneS_3)]Br$[5] or *fac*-$[Mn(CO)_3([10]aneS_3)]Br$ respectively as yellow solids in high yield. The new tripodal tritelluroether, $MeC(CH_2TePh)_3$ was obtained in moderate yield by treatment of $MeC(CH_2Br)_3$ with three molar equivalents of PhTeLi. The compounds *fac*-$[Mn(CO)_3(L)]CF_3SO_3$ (L = $MeS(CH_2)_2S(CH_2)_2SMe$, $MeSe(CH_2)_3Se(CH_2)_3SeMe$, $MeC(CH_2SMe)_3$, $MeC(CH_2SeMe)_3$, $MeC(CH_2TeMe)_3$, $MeC(CH_2TePh)_3$, $MeC(CH_2PPh_2)_3$, $MeC(CH_2AsMe_2)_3$ or $Ph_2P(CH_2)_2PPh(CH_2)_2PPh_2$) are readily produced by treatment of *fac*-$[Mn(CO)_3(Me_2CO)_3]CF_3SO_3$ (generated *in situ* from $[MnCl(CO)_5]$ and $AgCF_3SO_3$ in refluxing acetone[11]) with L at room temperature in Me_2CO solution. The compounds are all pale yellow solids, except when

Table 1 IR and NMR spectroscopic data

Compound	$\tilde{\nu}$(CO)/cm^{-1} [a]	δ^{31}P-{^{1}H} [b]	δ^{55}Mn ($w_{1/2}$/Hz) [b]	δ^{77}Se-{^{1}H} [b]	δ^{125}Te-{^{1}H} [b]
fac-[Mn(CO)$_3$([9]aneS$_3$)]Br	2045, 1957 [c]	—	−963 (120)	—	—
fac-[Mn(CO)$_3$([10]aneS$_3$)]Br	2045, 1957 [c]	—	−764 (550)	—	—
fac-[Mn(CO)$_3${MeS(CH$_2$)$_2$S(CH$_2$)$_2$SMe}]CF$_3$SO$_3$	2047, 1968	—	−696 (3500), −712 (sh)	—	—
fac-[Mn(CO)$_3${MeC(CH$_2$SMe)$_3$}]CF$_3$SO$_3$	2048, 1968	—	−477 (5000)	—	—
fac-[Mn(CO)$_3${MeC(CH$_2$SeMe)$_3$}]CF$_3$SO$_3$	2039, 1962	—	−721 (3610)	48	—
fac-[Mn(CO)$_3${MeSe(CH$_2$)$_3$Se(CH$_2$)$_3$SeMe}]CF$_3$SO$_3$	2029, 1945	—	−560 (2540)	48, 84	—
fac-[Mn(CO)$_3${MeC(CH$_2$TeMe)$_3$}]CF$_3$SO$_3$	2023, 1947	—	−1509 (1200)	—	112
fac-[Mn(CO)$_3${MeC(CH$_2$TePh)$_3$}]CF$_3$SO$_3$	2028, 1959	—	−1320 (2100)	—	353
fac-[Mn(CO)$_3$(PPh$_2$H)$_3$]CF$_3$SO$_3$	2019, 1946	34.0	−1830 (br q)	—	—
fac-[Mn(CO)$_3$(PCy$_2$H)$_3$]CF$_3$SO$_3$	2023, 1945	31.2	−1788 (1800)	—	—
fac-[Mn(CO)$_3$(PPhH$_2$)$_3$]CF$_3$SO$_3$	2041, 1963	−23.0	−1899 (q, ^1J *ca.* 190 Hz)	—	—
fac-[Mn(CO)$_3${MeC(CH$_2$PPh$_2$)$_3$}]CF$_3$SO$_3$	2030, 1960	29.9	−1798 (q, ^1J *ca.* 200 Hz)	—	—
fac-[Mn(CO)$_3${Ph$_2$P(CH$_2$)$_2$PPh(CH$_2$)$_2$PPh$_2$}]CF$_3$SO$_3$	2028, 1959	110.4, 71.5	−1950 (1500)	—	—
fac-[Mn(CO)$_3${MeC(CH$_2$AsMe$_2$)$_3$}]CF$_3$SO$_3$	2024, 1949	—	−1857 (600)	—	—
fac-[Re(CO)$_3${MeC(CH$_2$SeMe)$_3$}]CF$_3$SO$_3$	2044, 1952	—	—	22.7	—

[a] In Me_2CO. [b] Spectra were recorded in CH_2Cl_2–$CDCl_3$ unless otherwise stated. [c] Solution in dmf.

L = MeSe(CH$_2$)$_3$Se(CH$_2$)$_3$SeMe which is a yellow-orange oil. Similar reactions using three molar equivalents of PCy$_2$H, PPh$_2$H or PPhH$_2$ (L) yield *fac*-[Mn(CO)$_3$(L)$_3$]CF$_3$SO$_3$ as pale yellow solids. These monodentate phosphines show a significant decrease in cone angle from PCy$_2$H ⟶ PPh$_2$H ⟶ PPhH$_2$, and the *fac*-[Mn(CO)$_3$(L)$_3$]$^+$ cations are expected to show almost regular C_{3v} symmetry (see below). The compound *fac*-[Re(CO)$_3${MeC(CH$_2$SeMe)$_3$}]CF$_3$SO$_3$ was prepared *via* a similar procedure, although we were unable to obtain [Re(CO)$_3${MeC(CH$_2$TeMe)$_3$}]CF$_3$SO$_3$ in a pure form. While the ligand architecture of the tripodal ligands means that only the *fac* isomer is possible for their mononuclear complexes, either *fac* or *mer* isomers are possible in the other systems. In each case the reaction was monitored by solution IR spectroscopy which showed gradual loss of the bands due to the tris(acetone) manganese(I) precursor and the appearance of two new bands associated with the product, indicative of a *fac*-tricarbonyl unit (a_1 + e). The IR data are presented in Table 1 and the numerical figures reveal a shift in both the a_1 and e modes to low frequency according to the donor atom type, S ⟶ Se ⟶ Te ≈ P ≈ As, suggesting increased back bonding to CO along this series. Uson *et al.*[11] have described the synthesis of a range of *mer*- and *fac*-[Mn(CO)$_3$L$_3$]$^+$ species where L is a tertiary phosphine and Carriedo *et al.*[12] have reported the preparations of a series of cationic manganese(I) complexes involving PPh$_2$H, including *fac*-[Mn(CO)$_3$(PPh$_2$H)$_3$]$^+$. The ν(CO) data for these species are comparable with those from our primary and secondary phosphine compounds. Electrospray mass spectra (MeCN) for the products show peaks with the correct isotopic distribution for [Mn(CO)$_3$(L)]$^+$ or, in the case of the monodentate phosphine complexes, [Mn(CO)$_3$L$_3$]$^+$ (L = PPh$_2$H, PCy$_2$H or PPhH$_2$).

NMR spectroscopy

The ^{1}H, ^{13}C-{^{1}H}, ^{31}P-{^{1}H}, ^{55}Mn, ^{77}Se-{^{1}H} and ^{125}Te-{^{1}H} NMR spectra were recorded for the compounds where appropriate. The ^{1}H NMR spectra are not very informative, the resonances associated with the ligands being broadened by the ^{55}Mn quadrupole. In the primary and secondary phosphine complexes the PH protons appear as a broadened, widely separated ($^1J_{PH}$ *ca.* 300 Hz) multiplet. ^{13}C-{^{1}H} NMR spectroscopy confirms the presence of the Group 15 or 16 donor ligand and also shows a single broad δ(CO) resonance. In the case of *fac*-[Mn(CO)$_3$([9]aneS$_3$)]$^+$ coupling of δ(CO) to ^{55}Mn is also observed giving a 1:1:1:1:1:1 sextet with $^1J_{MnC}$ *ca.* 160 Hz. The manganese(I) species [Mn(RNC)$_6$]$^+$ (R = Me, Et, Pr^i, Bu^t or cyclohexyl) which involve π-acceptor isocyanide ligands rather than CO, show $^1J_{MnC}$ = 111–121 Hz.[13] The observation of ^{55}Mn–^{13}C coupling for [Mn(CO)$_3$([9]aneS$_3$)]$^+$ indicates that the electric field gradient at the Mn nucleus in this species is very close to zero, since otherwise the large quadrupole moment associated with ^{55}Mn (I = 5/2, 100%, $Q = 0.55 \times 10^{-28}$ m^2) would be expected to lead to significant broadening of the directly bonded δ(CO) resonance.[14] A very broad δ(CO) multiplet is also observed for [Mn(CO)$_3${MeC(CH$_2$PPh$_2$)$_3$}]$^+$ and for the tris-primary and -secondary phosphine complexes, all of which have almost regular C_{3v} symmetry.

The ^{125}Te-{^{1}H} NMR spectrum of [Mn(CO)$_3${MeC(CH$_2$TeMe)$_3$}]CF$_3$SO$_3$ shows a single resonance at δ 112, indicative of three equivalent Te donors and hence *fac*-tridentate co-ordination in solution (free MeC(CH$_2$TeMe)$_3$ δ^{125}Te 21). Since pyramidal inversion at a co-ordinated Te donor atom is expected to be slow on the NMR timescale,[1] this also implies that the ligand is in the *syn* configuration, with all three terminal Me groups pointing in the same direction giving a propeller-like arrangement. The ^{13}C-{^{1}H} and ^{1}H NMR spectra confirm the *syn* assignment. The *syn* isomer also occurs for *fac*-[M(CO)$_3${MeC(CH$_2$SeMe)$_3$}]CF$_3$SO$_3$: M = Mn, δ(^{77}Se) = 48; M = Re, δ(^{77}Se) = 23. The δ(^{125}Te):δ(^{77}Se) ratio for the manganese species of *ca.* 2.3:1 is considerably higher than the more usual[15] 1.7–1.8:1 and this suggests that there is a considerable increase in electron density at the Mn in the cationic tritelluroether complex compared to the selenoether analogue. The manganese(I) complex of the new Ph-substituted tritelluroether, [Mn(CO)$_3${MeC(CH$_2$TePh)$_3$}]CF$_3$SO$_3$, also shows a singlet at δ(^{125}Te) = 353 (free MeC(CH$_2$TePh)$_3$ δ 387). The compound *fac*-[Mn(CO)$_3${MeSe(CH$_2$)$_3$Se(CH$_2$)$_3$SeMe}]$^+$ shows two δ(^{77}Se) resonances 48 and 84 assigned to CH$_2$Se and MeSe respectively.

For the phosphine complexes ^{31}P-{^{1}H} NMR spectroscopy confirms the *fac* arrangement, δ(^{31}P) showing a very significant high frequency co-ordination shift. The resonances are broadened due to the directly bonded quadrupolar Mn, and for some of the monodentate phosphine complexes there is some evidence of coupling to ^{55}Mn giving a six line pattern. The compound *fac*-[Mn(CO)$_3${Ph$_2$P(CH$_2$)$_2$PPh(CH$_2$)$_2$PPh$_2$}]$^+$ shows two ^{31}P resonances at δ 110.4 and 71.5 assigned to the central PPh and terminal PPh$_2$ functions respectively and consistent with the presence of 5-membered chelate rings.[16]

We have shown previously that ^{55}Mn NMR is a sensitive probe of subtle differences in bonding in Group 15 and 16 ligand complexes of manganese(I) carbonyl halides.[4,5] We have conducted similar studies on the cationic species in this work to enable comparisons to be made between the neutral carbonyl halide derivatives and the cationic species reported here. Some interesting trends become apparent. The ^{55}Mn NMR spectrum of [Mn(CO)$_3$([9]aneS$_3$)]$^+$ shows a single sharp resonance at δ −963. The linewidth of 120 Hz compares with $w_{1/2}$ of 1000–3000 Hz for [MnX(CO)$_3$(dithioether)], and indicates that in the

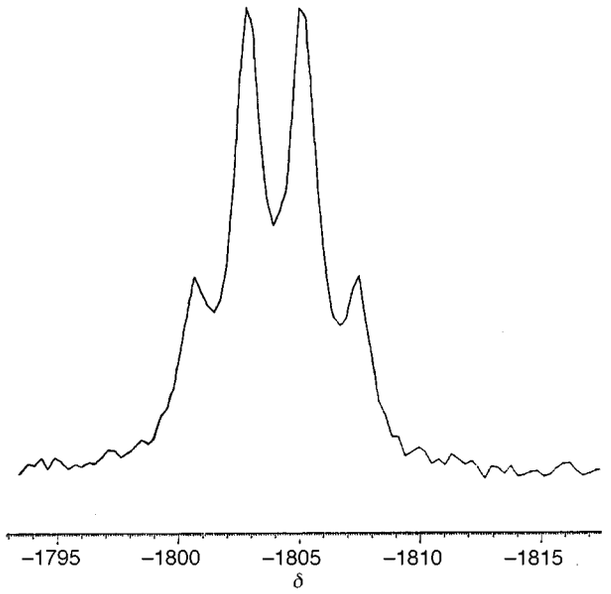

Fig. 1 The ^{55}Mn NMR spectrum of *fac*-[Mn(CO)$_3${MeC(CH$_2$PPh$_2$)$_3$}]-CF$_3$SO$_3$ (89.27 MHz, CH$_2$Cl$_2$–CDCl$_3$).

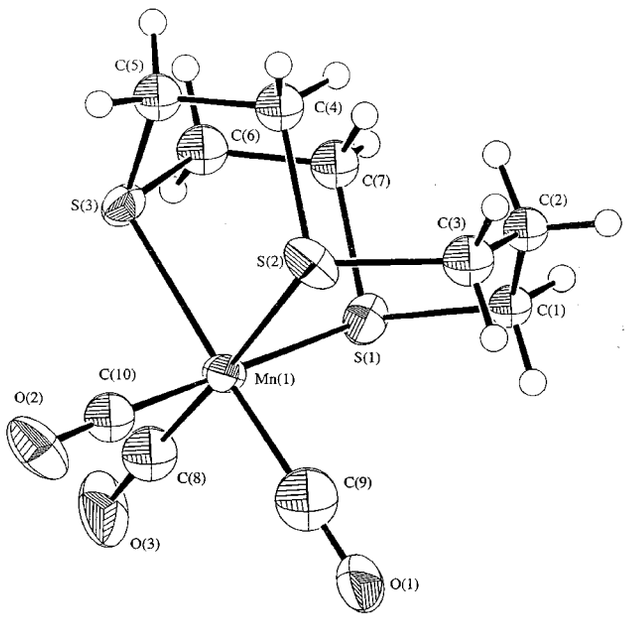

Fig. 2 View of the structure of one of the two independent [Mn(CO)$_3$-([10]aneS$_3$)]$^+$ cations with the numbering scheme adopted (the other cation showed some disorder, see Experimental section). Ellipsoids are drawn at the 40% probability level.

former (C_{3v}) species the electric field gradient at the Mn is very close to zero. Substitution of [9]aneS$_3$ by [10]aneS$_3$ results in a high frequency shift and a slight broadening of the signal due to the reduction in symmetry caused by the presence of two 5-membered and one 6-membered chelate ring. This trend is continued for the less symmetrical species *fac*-[Mn(CO)$_3$-{MeS(CH$_2$)$_2$S(CH$_2$)$_2$SMe}]$^+$. Its spectrum shows two signals assigned to the presence of two invertomers and indicating that pyramidal inversion is slow on the NMR timescale. The chemical shifts for these trithioether ligand complexes are all to low frequency of those of [MnX(CO)$_3$(dithioether)] (δ +67 to −537).[4] Within this series of trithioether species we oberve a variation in δ(^{55}Mn) with chelate ring size. Thus those species with 5-membered chelate rings are more highly shielded than those with 6-membered rings, a similar trend to that observed in related diphosphine complexes.[5] For the homologous series *fac*-[Mn(CO)$_3${MeC(CH$_2$EMe)$_3$}]CF$_3$SO$_3$, all of which exist in solution principally as the *syn* isomer, there is a very noticeable low frequency shift down the series δ(^{55}Mn) −477 (E = S), −721 (E = Se) and −1509 (E = Te), while [Mn(CO)$_3${MeC(CH$_2$TePh)$_3$}]CF$_3$SO$_3$ gives δ(^{55}Mn) = −1320, *i.e.* more deshielded than for the Me-substituted analogue, indicating that the Ph-substituted ligand is a poorer σ donor compared to the methyl analogue.

Comparing the data for the cationic complexes with those for the neutral species reported previously we find that δ(^{55}Mn) follows the same trend with donor type showing a shift to low frequency along the series S ⟶ Se ⟶ Te, although for a donor type δ(^{55}Mn) for the cationic species here are considerably to low frequency of the neutral species. These trends may be attributed to (i) increased E→Mn σ donation down Group 16 and (ii) enhanced E→Mn σ donation in the cationic species as a consequence of the positive charge on the Mn. In our previous work we have shown that for the neutral Group 15 complexes *fac*-[MnX(CO)$_3$(L–L)] (L–L = diphosphine, diarsine or distibine) there is a small shift in δ(^{55}Mn) to low frequency down the group.[5] For the cationic phosphine and arsine complexes in this study we find δ(^{55}Mn) *ca.* −1750, *i.e.* to low frequency of that of even the tripodal telluroether species [Mn(CO)$_3${MeC(CH$_2$TeMe)$_3$}]$^+$. For the most symmetrical species [Mn(CO)$_3${MeC(CH$_2$PPh$_2$)$_3$}]CF$_3$SO$_3$ and [Mn(CO)$_3$-(PPhH$_2$)$_3$]CF$_3$SO$_3$ coupling is seen, giving a quartet with $^1J_{MnP}$ *ca.* 200 and 190 respectively (Fig. 1), while broadened, partially collapsed quartets are observed for [Mn(CO)$_3$(PPh$_2$H)$_3$]$^+$ and [Mn(CO)$_3$(PCy$_2$H)$_3$]$^+$. These observations contrast with those for the neutral species [MnX(CO)$_3$(diphosphine)] where no ^{55}Mn–^{31}P coupling is seen in any case, reflecting the much lower symmetry at Mn. The tris(diphosphine) species [Mn{Me$_2$P-(CH$_2$)$_2$PMe$_2$}$_3$]$^+$, which is clearly much closer to octahedral symmetry than the tricarbonyl derivatives, shows $^1J_{MnP}$ = 242 Hz.[17] Comparing the shifts for the cationic species with those for the neutral [MnX(CO)$_3$(diphosphine)] we again find that δ(^{55}Mn) for the cationic species are significantly to lower frequency.

Crystallographic studies

Other than *fac*-[Mn(CO)$_3${MeC(CH$_2$TeMe)$_3$}]CF$_3$SO$_3$, the structure of which we have communicated,[7] a search of the Cambridge Crystallographic Database revealed that the only structurally characterised species of the form *fac*-[Mn(CO)$_3$-(L$_3$)]$^+$, where L$_3$ is a tridentate thio-, seleno- or telluro-ether, phosphine or arsine, is *fac*-[Mn(CO)$_3$([9]aneS$_3$)]$^+$.[6] Thus we have undertaken structural analyses on several of the compounds reported here. Crystals were obtained by vapour diffusion of diethyl ether or light petroleum (bp 40–60 °C) into solutions of the complexes in CH$_2$Cl$_2$, although recrystallisation of [Mn(CO)$_3$([10]aneS$_3$)]Br from CH$_2$Cl$_2$–diethyl ether yields pale yellow crystals of [Mn(CO)$_3$([10]aneS$_3$)]$_2$[MnBr$_4$]. The structure shows two independent cations (Fig. 2, Table 2) and one dianion in the asymmetric unit. The [Mn(CO)$_3$-([10]aneS$_3$)]$^+$ cations show a distorted octahedral geometry with the three CO ligands occupying mutually *fac* co-ordination sites and the thioether ligand tridentate, Mn–S 2.303(5)–2.405(6) Å. The S–Mn–S angles involved in the 6-membered chelate rings are considerably larger than those in the 5-membered chelate rings, consistent with the more restricted bite angle of the dithioether unit in the latter. The data for [Mn(CO)$_3${Me-S(CH$_2$)$_2$S(CH$_2$)$_2$SMe}]CF$_3$SO$_3$ were rather weak and hence the residuals are higher than normally expected. The structure of the cation shows (Fig. 3, Table 3) the trithioether binding facially to Mn^I with three CO ligands completing the distorted octahedral geometry, Mn–S 2.320(3)–2.402(4) Å. The S–Mn–S angles involved in the 5-membered chelate-rings are 85.73(10) and 88.16(10)°. The Mn–S distances in these compounds compare well with those observed by Wieghardt and co-workers[6] for [Mn(CO)$_3$([9]aneS$_3$)]$_3$[PF$_6$]$_2$Br·2 H$_2$O, d(Mn–S) = 2.314(4)–2.341(4) Å, and with those observed for the neutral

Table 2 Selected bond lengths (Å) and angles (°) for $[Mn(CO)_3([10]aneS_3)]^+$

Br(1)–Mn(3)	2.510(3)	Br(2)–Mn(3)	2.505(3)
Br(3)–Mn(3)	2.528(3)	Br(4)–Mn(3)	2.513(3)
Mn(1)–S(1)	2.338(5)	Mn(1)–S(2)	2.343(5)
Mn(1)–S(3)	2.303(5)	Mn(1)–C(8)	1.79(2)
Mn(1)–C(9)	1.77(2)	Mn(1)–C(10)	1.82(2)
Mn(2)–S(4)	2.339(6)	Mn(2)–S(5)	2.405(6)
Mn(2)–S(6)	2.325(5)	Mn(2)–C(18)	1.83(2)
Mn(2)–C(19)	1.80(2)	Mn(2)–C(20)	1.78(2)
S(1)–Mn(1)–S(2)	93.4(2)	S(1)–Mn(1)–S(3)	87.7(2)
S(1)–Mn(1)–C(8)	88.7(6)	S(1)–Mn(1)–C(9)	90.7(7)
S(1)–Mn(1)–C(10)	178.0(6)	S(2)–Mn(1)–S(3)	86.4(2)
S(2)–Mn(1)–C(8)	176.9(6)	S(2)–Mn(1)–C(9)	91.9(7)
S(2)–Mn(1)–C(10)	88.6(6)	S(3)–Mn(1)–C(8)	91.4(6)
S(3)–Mn(1)–C(9)	177.6(7)	S(3)–Mn(1)–C(10)	92.0(6)
C(8)–Mn(1)–C(9)	90.3(9)	C(8)–Mn(1)–C(10)	89.3(8)
C(9)–Mn(1)–C(10)	89.7(9)	S(4)–Mn(2)–S(5)	95.3(2)
S(4)–Mn(2)–S(6)	87.9(2)	S(4)–Mn(2)–C(18)	177.2(6)
S(4)–Mn(2)–C(19)	87.5(6)	S(4)–Mn(2)–C(20)	92.7(7)
S(5)–Mn(2)–S(6)	84.5(2)	S(5)–Mn(2)–C(18)	87.3(6)
S(5)–Mn(2)–C(19)	175.8(6)	S(5)–Mn(2)–C(20)	91.4(7)
S(6)–Mn(2)–C(18)	91.3(6)	S(6)–Mn(2)–C(19)	92.5(6)
S(6)–Mn(2)–C(20)	175.9(7)	C(18)–Mn(2)–C(19)	89.8(8)
C(18)–Mn(2)–C(20)	88.3(9)	C(19)–Mn(2)–C(20)	91.5(9)

Table 3 Selected bond lengths (Å) and angles (°) for $[Mn(CO)_3\{MeS(CH_2)_2S(CH_2)_2SMe\}]^+$

Mn(1)–S(1)	2.352(3)	Mn(1)–S(2)	2.320(3)
Mn(1)–S(3)	2.402(4)	Mn(1)–C(1)	1.82(1)
Mn(1)–C(2)	1.797(10)	Mn(1)–C(3)	1.804(10)
S(1)–Mn(1)–S(2)	88.16(10)	S(1)–Mn(1)–S(3)	85.2(1)
S(1)–Mn(1)–C(1)	92.7(3)	S(1)–Mn(1)–C(2)	89.8(3)
S(1)–Mn(1)–C(3)	178.3(3)	S(2)–Mn(1)–S(3)	85.73(10)
S(2)–Mn(1)–C(1)	93.1(3)	S(2)–Mn(1)–C(2)	175.7(3)
S(2)–Mn(1)–C(3)	90.5(3)	S(3)–Mn(1)–C(1)	177.6(3)
S(3)–Mn(1)–C(2)	90.4(3)	S(3)–Mn(1)–C(3)	93.6(3)
C(1)–Mn(1)–C(2)	90.7(4)	C(1)–Mn(1)–C(3)	88.5(4)
C(2)–Mn(1)–C(3)	91.5(4)		

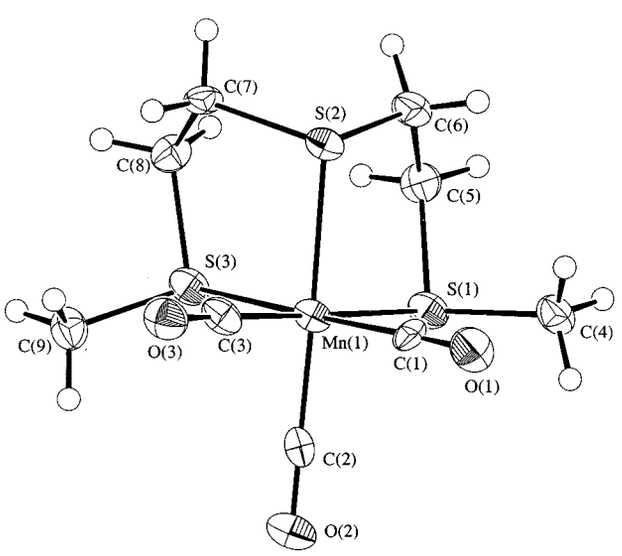

Fig. 3 View of the structure of $[Mn(CO)_3\{MeS(CH_2)_2S(CH_2)_2SMe\}]^+$ with the numbering scheme adopted. Ellipsoids are drawn at the 40% probability level.

manganese(I) thioether species *fac*-$[MnCl(CO)_3\{PhS(CH_2)_2SPh\}]$ (Mn–S 2.362(2) Å) and *fac*-$[MnCl(CO)_3\{MeS(CH_2)_2SMe\}]$ (Mn–S 2.3698(9), 2.3633(9) Å).[4] The structures of $[Mn(CO)_3\{MeC(CH_2SMe)_3\}]CF_3SO_3$ and $[Mn(CO)_3\{MeC(CH_2SeMe)_3\}]CF_3SO_3$ show (Figs. 4 and 5, Tables 4 and 5) a facially bound tripodal ligand in the *syn* form, with the Me substituents adopting a propeller-like arrangement (this is consistent with the isomer observed in solution by NMR spectroscopy), Mn–S 2.3481(8)–2.3579(8), Mn–Se 2.449(1)–2.464(1) Å. The S–Mn–S angles lie in the range 88.12(3)–91.63(3)°, while the Se–Mn–Se angles are 89.18(4)–91.45(4)°. The compound $[Re(CO)_3\{MeC(CH_2SeMe)_3\}]CF_3SO_3$ adopts a very similar arrangment (Fig. 6, Table 6), the selenoether again adopting the *syn* form, Re–Se 2.579(3)–2.594(2) Å. The Se–Re–Se angles lie in the range 87.09(8)–89.08(8)°. These are the first cationic manganese(I) and rhenium(I) selenoether complexes, although the M–Se bond lengths can be compared with those in the neutral *fac*-$[MnCl(CO)_3\{MeSe(CH_2)_2SeMe\}]$ (Mn–Se 2.481(3), 2.467(3) Å), *fac*-$[MnCl(CO)_3\{MeSe(CH_2)_3SeMe\}]$ (Mn–Se 2.474(2), 2.482(2) Å)[4] and *fac*-$[ReI(CO)_3(MeSeCH_2CH_2SeMe)]$ (Re–Se 2.593(1), 2.597(1) Å).[18] The structure of *fac*-$[Mn(CO)_3\{MeC(CH_2TeMe)_3\}]CF_3SO_3$ shows

Table 4 Selected bond lengths (Å) and angles (°) for $[Mn(CO)_3\{MeC(CH_2SMe)_3\}]^+$

Mn(1)–S(1)	2.3579(8)	Mn(1)–S(2)	2.3481(8)
Mn(1)–S(3)	2.3487(9)	Mn(1)–C(18)	1.816(3)
Mn(1)–C(20)	1.806(3)	Mn(1)–C(26)	1.805(3)
S(1)–Mn(1)–S(2)	88.12(3)	S(1)–Mn(1)–S(3)	88.77(3)
S(1)–Mn(1)–C(18)	175.40(10)	S(1)–Mn(1)–C(20)	88.90(9)
S(1)–Mn(1)–C(26)	93.44(10)	S(2)–Mn(1)–S(3)	91.63(3)
S(2)–Mn(1)–C(18)	93.45(9)	S(2)–Mn(1)–C(20)	175.83(10)
S(2)–Mn(1)–C(26)	88.19(9)	S(3)–Mn(1)–C(18)	86.87(10)
S(3)–Mn(1)–C(20)	91.2(1)	S(3)–Mn(1)–C(26)	177.77(10)
C(18)–Mn(1)–C(20)	89.8(1)	C(18)–Mn(1)–C(26)	90.9(1)
C(20)–Mn(1)–C(26)	89.1(1)		

Table 5 Selected bond lengths (Å) and angles for (°) $[Mn(CO)_3\{MeC(CH_2SeMe)_3\}]^+$

Se(1)–Mn(1)	2.464(1)	Se(2)–Mn(1)	2.459(1)
Se(3)–Mn(1)	2.449(1)	Mn(1)–C(1)	1.821(8)
Mn(1)–C(2)	1.793(8)	Mn(1)–C(3)	1.804(8)
Se(1)–Mn(1)–Se(2)	89.19(5)	Se(1)–Mn(1)–Se(3)	89.18(4)
Se(1)–Mn(1)–C(1)	175.3(2)	Se(1)–Mn(1)–C(2)	93.5(2)
Se(1)–Mn(1)–C(3)	87.6(2)	Se(2)–Mn(1)–Se(3)	91.45(4)
Se(2)–Mn(1)–C(1)	86.5(2)	Se(2)–Mn(1)–C(2)	177.2(2)
Se(2)–Mn(1)–C(3)	90.8(3)	Se(3)–Mn(1)–C(1)	92.7(2)
Se(3)–Mn(1)–C(2)	87.7(2)	Se(3)–Mn(1)–C(3)	176.0(2)
C(1)–Mn(1)–C(2)	90.9(3)	C(1)–Mn(1)–C(3)	90.7(3)
C(2)–Mn(1)–C(3)	90.2(4)		

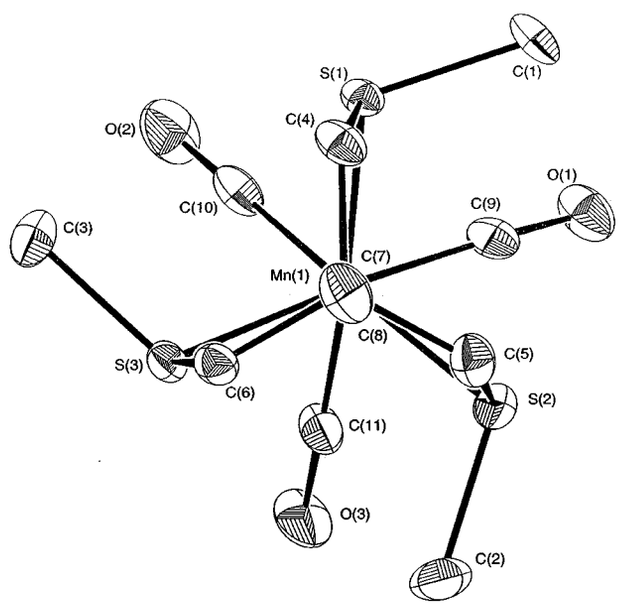

Fig. 4 View of the structure of $[Mn(CO)_3\{MeC(CH_2SMe)_3\}]^+$. Details as in Fig. 3.

Table 6 Selected bond lengths (Å) and angles (°) for $[Re(CO)_3\{MeC(CH_2SeMe)_3\}]^+$

Re(1)–Se(1)	2.588(3)	Re(1)–Se(2)	2.579(2)
Re(1)–Se(3)	2.587(2)	Re(1)–C(1)	1.91(2)
Re(1)–C(2)	1.86(2)	Re(1)–C(3)	1.86(3)
Re(2)–Se(4)	2.579(3)	Re(2)–Se(5)	2.594(2)
Re(2)–Se(6)	2.578(3)	Re(2)–C(4)	1.93(3)
Re(2)–C(5)	1.98(3)	Re(2)–C(6)	1.95(3)
Se(1)–Re(1)–Se(2)	87.94(8)	Se(1)–Re(1)–Se(3)	87.96(8)
Se(1)–Re(1)–C(1)	87.2(7)	Se(1)–Re(1)–C(2)	91.2(7)
Se(1)–Re(1)–C(3)	177.4(6)	Se(2)–Re(1)–Se(3)	87.76(7)
Se(2)–Re(1)–C(1)	91.9(6)	Se(2)–Re(1)–C(2)	178.6(6)
Se(2)–Re(1)–C(3)	89.7(6)	Se(3)–Re(1)–C(1)	175.1(7)
Se(3)–Re(1)–C(2)	91.1(7)	Se(3)–Re(1)–C(3)	90.9(6)
C(1)–Re(1)–C(2)	89.2(9)	C(1)–Re(1)–C(3)	94.0(9)
C(2)–Re(1)–C(3)	91.1(10)	Se(4)–Re(2)–Se(5)	87.68(8)
Se(4)–Re(2)–Se(6)	89.08(8)	Se(4)–Re(2)–C(4)	176.8(9)
Se(4)–Re(2)–C(5)	86.8(9)	Se(4)–Re(2)–C(6)	93.7(8)
Se(5)–Re(2)–Se(6)	87.09(8)	Se(5)–Re(2)–C(4)	89.9(7)
Se(5)–Re(2)–C(5)	94.2(6)	Se(5)–Re(2)–C(6)	176.1(7)
Se(6)–Re(2)–C(4)	92.9(10)	Se(6)–Re(2)–C(5)	175.6(9)
Se(6)–Re(2)–C(6)	89.3(7)	C(4)–Re(2)–C(5)	91(1)
C(4)–Re(2)–C(6)	88(1)	C(5)–Re(2)–C(6)	89.5(9)

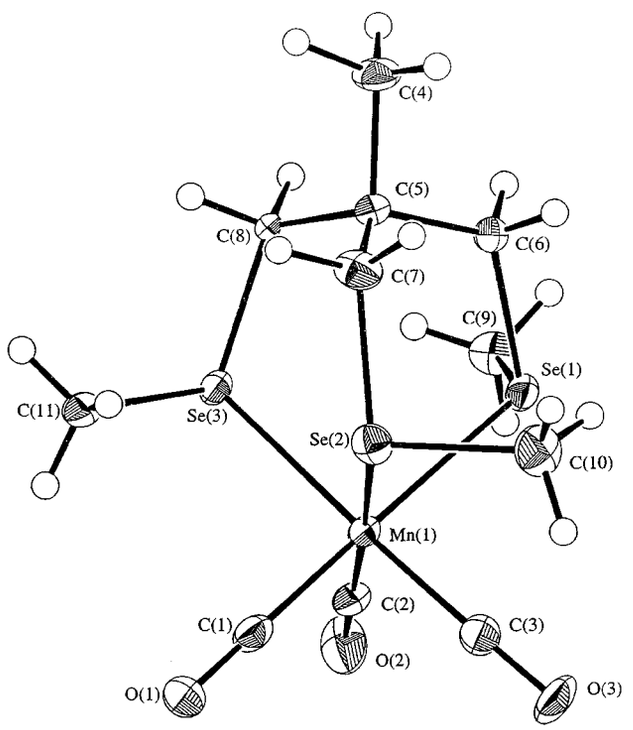

Fig. 5 View of the structure of $[Mn(CO)_3\{MeC(CH_2SeMe)_3\}]^+$. Details as in Fig. 3.

the Me substituents are disordered and this prevented us from being able to identify the configuration in the solid state (NMR studies show that only the *syn* isomer is present in solution).[7] Comparing the structural data for the homologous series $[Mn(CO)_3\{MeC(CH_2EMe)_3\}]^+$ shows an increase in *d*(Mn–E) according to the series S < Se < Te, in accord with the increasing covalent radii. In the absence of structural data on a much wider range of analogous systems, it is not possible to be certain whether the subtle changes in bonding down the group are reflected in the measured structural parameters; these are probably within the error limits of the X-ray analyses. In the Ph-substituted telluroether complex *fac*-$[Mn(CO)_3\{MeC(CH_2TePh)_3\}]CF_3SO_3$ the cation also adopts a distorted octahedral geometry (Fig. 7, Table 7), with Mn–Te 2.615(2)–2.643(2) Å, and the Ph groups adopt the *syn* form. Thus the Mn–Te distances in the Me-substituted species (2.601(1), 2.6063(8) Å) are shorter than those for the Ph-substituted analogue, consistent

Table 7 Selected bond lengths (Å) and angles (°) for $[Mn(CO)_3\{MeC(CH_2TePh)_3\}]^+$

Te(1)–Mn(1)	2.627(2)	Te(2)–Mn(1)	2.615(2)
Te(3)–Mn(1)	2.643(2)	Mn(1)–C(1)	1.80(1)
Mn(1)–C(2)	1.80(1)	Mn(1)–C(3)	1.83(1)
Te(1)–Mn(1)–Te(2)	87.68(6)	Te(1)–Mn(1)–Te(3)	86.07(6)
Te(1)–Mn(1)–C(1)	92.0(5)	Te(1)–Mn(1)–C(2)	175.6(4)
Te(1)–Mn(1)–C(3)	92.1(4)	Te(2)–Mn(1)–Te(3)	94.49(6)
Te(2)–Mn(1)–C(1)	176.7(5)	Te(2)–Mn(1)–C(2)	88.4(4)
Te(2)–Mn(1)–C(3)	87.1(4)	Te(3)–Mn(1)–C(1)	88.8(5)
Te(3)–Mn(1)–C(2)	92.4(4)	Te(3)–Mn(1)–C(3)	177.5(4)
C(1)–Mn(1)–C(2)	92.0(6)	C(1)–Mn(1)–C(3)	89.6(6)
C(2)–Mn(1)–C(3)	89.6(6)		

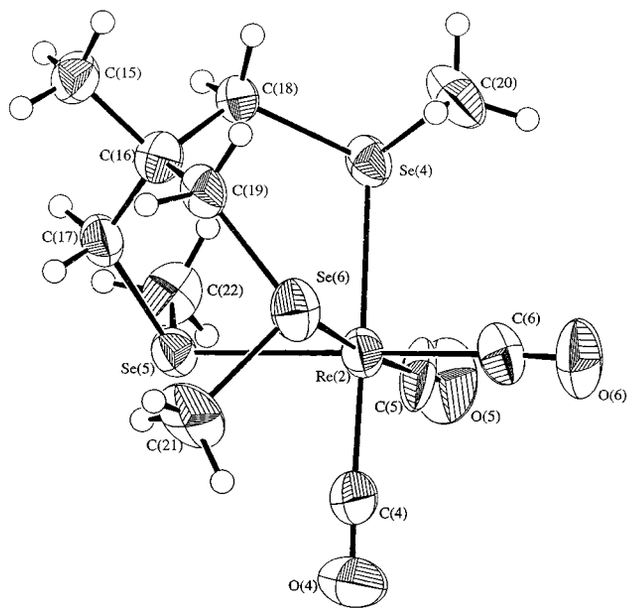

Fig. 6 View of the structure of one of the independent $[Re(CO)_3\{MeC(CH_2SeMe)_3\}]^+$ cations with the numbering scheme adopted (the other cation is essentially indistinguishable). Ellipsoids are drawn at the 40% probability level.

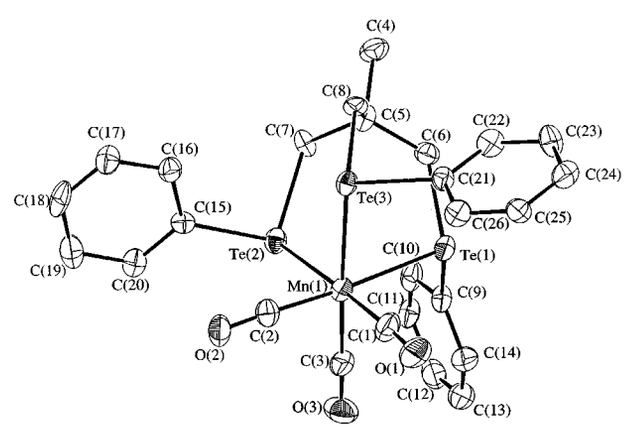

Fig. 7 View of the structure of $[Mn(CO)_3\{MeC(CH_2TePh)_3\}]^+$ with the numbering scheme adopted. Ellipsoids are drawn at the 40% probability level.

with the Me-substituted tripod being the better σ-donor ligand. These compounds represent the only two structurally characterised species involving a co-ordinated tritelluroether ligand. The crystal stucture of the triphosphine derivative $[Mn(CO)_3\{MeC(CH_2PPh_2)_3\}]CF_3SO_3$ confirms that within the cation the phosphine is bonded in a *fac*-tridentate fashion, consistent with the approximately C_{3v} structure deduced spectroscopically, giving a distorted octahedron (Fig. 8, Table 8), Mn–P 2.341(2)–2.359(2) Å. The P–Mn–P angles lie in the range 85.89(6)–89.14(6)°.

Table 8 Selected bond lengths (Å) and angles (°) for $[Mn(CO)_3\{MeC(CH_2PPh_2)_3\}]^+$

Mn(1)–P(1)	2.341(2)	Mn(1)–P(2)	2.359(2)
Mn(1)–P(3)	2.351(2)	Mn(1)–C(1)	1.822(7)
Mn(1)–C(2)	1.814(7)	Mn(1)–C(3)	1.819(7)
P(1)–Mn(1)–P(2)	85.94(6)	P(1)–Mn(1)–P(3)	89.14(6)
P(1)–Mn(1)–C(1)	176.8(2)	P(1)–Mn(1)–C(2)	91.4(2)
P(1)–Mn(1)–C(3)	93.8(2)	P(2)–Mn(1)–P(3)	85.89(6)
P(2)–Mn(1)–C(1)	95.9(2)	P(2)–Mn(1)–C(2)	177.1(2)
P(2)–Mn(1)–C(3)	94.3(2)	P(3)–Mn(1)–C(1)	88.4(2)
P(3)–Mn(1)–C(2)	93.0(2)	P(3)–Mn(1)–C(3)	177.1(2)
C(1)–Mn(1)–C(2)	86.8(3)	C(1)–Mn(1)–C(3)	88.7(3)
C(2)–Mn(1)–C(3)	87.0(3)		

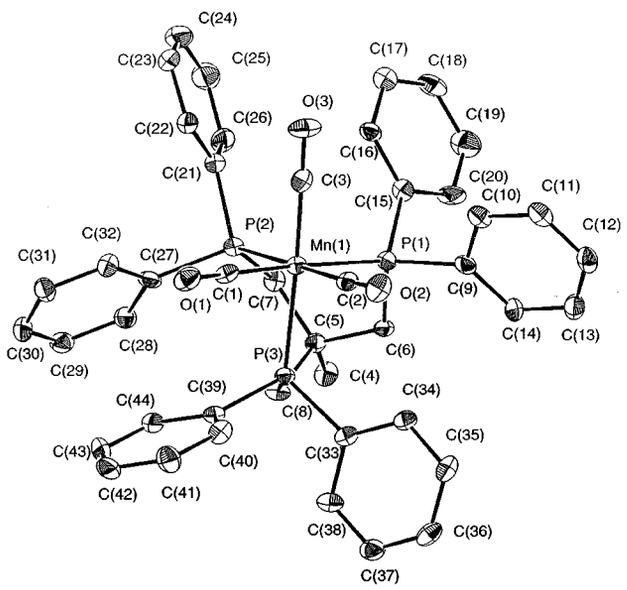

Fig. 8 View of the structure of $[Mn(CO)_3\{MeC(CH_2PPh_2)_3\}]^+$. Details as in Fig. 7.

These Mn–P distances are slightly longer than those observed in the neutral manganese(I) species, *e.g.* $[MnCl(CO)_3\{C_6H_4(PPh_2)_2\text{-}o\}]$ Mn–P 2.325(2), 2.320(2), $[MnCl\{C_6H_4(PH_2)_2\text{-}o\}]$ Mn–P 2.280(2), 2.281(2) and $[MnBr(CO)_3(PPhH_2)_2]$ Mn–P 2.305(1), 2.322(1) Å,[5] possibly reflecting the increased steric crowding in the cationic species.

Conclusion

These studies show that trisubstituted manganese(I)-tricarbonyl cations involving Group 15 and 16 donor ligands are readily accessible in good yields *via fac*-$[Mn(CO)_3(Me_2CO)_3]^+$, and several of these compounds have been structurally authenticated by single crystal X-ray diffraction studies. Manganese-55 NMR spectroscopy shows that for a given donor type $\delta(^{55}Mn)$ lies significantly to low frequency compared to those for the neutral $[MnX(CO)_3(L\text{–}L)]$ (X = Cl or Br), although the same trends in σ-donor capability with donor type are observed. The subtle dependence of the electric field gradient at the metal centre on the symmetry is clearly demonstrated, and notably for those species with C_{3v} symmetry the electric field gradient is sufficiently small such that coupling to other nuclei is clearly evident.

Experimental

Infrared spectra were measured as CsI discs using a Perkin-Elmer 983G spectrometer over the range 200–4000 cm^{-1} or in solution using a Perkin-Elmer 1600 FTIR spectrometer, mass spectra by positive electrospray (ES) using a VG Biotech Platform. The ^1H NMR spectra were recorded in $CDCl_3$ using a Bruker AM300 spectrometer operating at 300 MHz, $^{13}C\text{-}\{^1H\}$, $^{31}P\text{-}\{^1H\}$, ^{55}Mn, $^{77}Se\text{-}\{^1H\}$ and $^{125}Te\text{-}\{^1H\}$ NMR spectra in CH_2Cl_2 solution in 10 mm o.d. tubes containing *ca.* 10% $CDCl_3$, using a Bruker AM360 spectrometer operating at 90.6, 145.8, 89.3, 68.7 and 113.6 MHz and referenced to TMS, external 85% H_3PO_4, external aqueous $KMnO_4$, external neat Me_2Se and external neat Me_2Te respectively. The complex $[Cr(acac)_3]$ was added to the solutions to alleviate the slow relaxation associated with the δ(CO) resonances. Microanalyses were performed by the University of Strathclyde microanalytical service. The compounds $[Mn(CO)_3(Me_2CO)_3]\text{-}CF_3SO_3$,[10] $[Mn(CO)_3([9]aneS_3)]Br$,[6] $MeC(CH_2SMe)_3$,[19] $MeSe(CH_2)_3Se(CH_2)_3SeMe$,[20] $MeC(CH_2SeMe)_3$,[20] $MeC(CH_2TeMe)_3$[21] and $MeC(CH_2AsMe_2)_3$[22] were prepared by literature methods.

Preparations

All preparations were conducted using standard Schlenk techniques under a dinitrogen atmosphere.

$MeC(CH_2TePh)_3$. The compound $MeC(CH_2Br)_3$ (9.27 g, 0.03 mmol) was injected onto a frozen solution (−196 °C) of PhTeLi (0.18 mmol). The mixture was allowed to thaw and stirred at room temperature for 18 h and then refluxed for 1 h. After cooling, the mixture was hydrolysed (50 cm^3 water), separated and the aqueous layer extracted with Et_2O (4 × 25 cm^3). The combined extracts were dried over $MgSO_4$. The solvent was removed *in vacuo*, leaving a deep red oil which was recrystallised twice from light petroleum (bp 40–60 °C) to yield the product as an orange powder. Yield 2.5 g, 12%. FAB mass spectrum (3-nitrobenzyl alcohol matrix): found *m/z* = 684, 609, 479; calculated for $MeC(CH_2{}^{130}TePh)_3$ (L) *m/z* = 690, 613 (L − Ph), 483 (L − TePh). ^1H NMR: δ 7.15–7.78 (m, Ph, 15 H), 3.23 (*s*, CH_2, 6 H, $^1J_{TeC}$ 24 Hz) and 1.20 (*s*, Me, 3 H). $^{13}C\text{-}\{^1H\}$ NMR: δ 113, 128, 129, 139 (Ph), 39.7 (C), 28.7 (CH_3) and 26.1 (CH_2). $^{125}Te\text{-}\{^1H\}$ NMR: δ 387.

***fac*-$[Mn(CO)_3([10]aneS_3)]Br$.** The compound [10]$aneS_3$ (0.022 g, 0.11 mmol) was added to a solution of $[MnBr(CO)_5]$ (0.031 g, 0.11 mmol) in dmf (15 cm^3). The resulting mixture was stirred at room temperature for 24 h and the solution IR spectrum monitored until the reaction had gone to completion. Addition of diethyl ether (100 cm^3) gave a yellow precipitate. Filtration and subsequent recrystallisation from MeCN–Et_2O afforded a yellow solid (yield 0.018 g, 38%). Found: C, 28.7, H, 3.3 $C_{10}H_{14}BrMnO_3S_3$ requires C, 29.0, H, 3.4%. Electrospray mass spectrum (MeCN): found *m/z* = 333, 346; calc. for $[Mn(CO)_3([10]aneS_3)]^+$ *m/z* = 333, $[Mn(CO)_2([10]aneS_3)\cdot MeCN]^+$ *m/z* = 346. ^1H NMR: δ 2.60–3.30 (m, CH_2). $^{13}C\text{-}\{^1H\}$ NMR: δ 209.8–220.3 (CO), 23.0, 18.8 (SCH_2) and 14.0 ($CH_2CH_2CH_2$).

***fac*-$[Mn(CO)_3\{MeS(CH_2)_2S(CH_2)_2SMe\}]CF_3SO_3$.** The compound $[MnBr(CO)_5]$ (0.073 g, 0.27 mmol) and $AgCF_3SO_3$ (0.068 g, 0.27 mmol) were dissolved in acetone (40 cm^3) and stirred at 60 °C for 1 h. The reaction was monitored by solution IR spectroscopy to give *fac*-$[Mn(CO)_3(Me_2CO)_3]^+$. The AgBr precipitate was filtered off, $MeS(CH_2)_2S(CH_2)_2SMe$ (0.048 g, 0.27 mmol) added and the mixture refluxed for 20 min and stirred at room temperature for 18 h. The reaction mixture was then evaporated to dryness and the product recrystallised from CH_2Cl_2–Et_2O to afford a yellow solid (yield 0.051 g, 41%). Required for $C_{10}H_{14}F_3MnO_6S_4\cdot CH_2Cl_2$: C, 23.8; H, 2.5. Found: C, 23.5; H, 3.2%. Electrospray mass spectrum (MeCN): found *m/z* = 334, 321, 293, 278, 265; calc. for $[Mn(CO)_3\{MeS(CH_2)_2S(CH_2)_2SMe\}.MeCN]^+$ *m/z* = 334, $[Mn(CO)_3\{MeS(CH_2)_2S(CH_2)_2SMe\}]^+$ *m/z* = 322, $[Mn(CO)_2\{MeS(CH_2)_2S(CH_2)_2SMe\}]^+$ *m/z* = 294, $[Mn\{MeS(CH_2)_2S(CH_2)_2SMe\}\cdot MeCN]^+$ *m/z* = 279, $[Mn(CO)\{MeS(CH_2)_2S(CH_2)_2SMe\}]^+$ *m/z* = 266. ^1H NMR: δ 1.9–3.5 (br, m). $^{13}C\text{-}\{^1H\}$ NMR: δ 212.2–219.6 (CO), 39.0, 36.6 (CH_2) and 22.1 (Me).

***fac*-[Mn(CO)$_3${MeSe(CH$_2$)$_3$Se(CH$_2$)$_3$SeMe}]CF$_3$SO$_3$.** Yield 40%. Electrospray mass spectrum (MeCN): found *m*/*z* = 492; calc. for [Mn(CO)$_3${Me^{80}Se(CH$_2$)$_3$^{80}Se(CH$_2$)$_3$^{80}SeMe}]$^+$ *m*/*z* = 493. ^{1}H NMR: δ 2.0–3.2 (m, CH$_2$ and CH$_3$). ^{13}C-{^{1}H} NMR: δ 215.0–223.1 (CO), 30.0 (CH$_2$*C*H$_2$CH$_2$), 26.2, 25.0 (CH$_2$Se) and 14.6 (MeSe).

***fac*-[Mn(CO)$_3${MeC(CH$_2$SMe)$_3$}]CF$_3$SO$_3$.** Yield 65%. Calc. for C$_{12}$H$_{18}$F$_3$MnO$_6$S$_4$·CH$_2$Cl$_2$: C, 26.8; H, 3.4. Found: C, 27.0; H, 3.5%. Electrospray mass spectrum (MeCN): found *m*/*z* = 349, calc. for [Mn(CO)$_3${MeC(CH$_2$SMe)$_3$}]$^+$ *m*/*z* = 349. ^{1}H NMR: δ 2.9 (*s*, CH$_2$, 6 H), 2.2 (*s*, SMe, 9 H) and 1.15 (*s*, CMe, 3 H). ^{13}C-{^{1}H} NMR: δ 214.0–217.1 (CO), 39.4 (SCH$_2$), 36.2 (C), 31.2 (CH$_3$) and 25.5 (SCH$_3$).

***fac*-[Mn(CO)$_3${MeC(CH$_2$SeMe)$_3$}]CF$_3$SO$_3$.** Yield 47%. Calc. for C$_{12}$H$_{18}$F$_3$MnO$_6$SSe$_3$: C, 22.5; H, 2.8. Found: C, 23.2; H, 3.0%. Electrospray mass spectrum (MeCN): found *m*/*z* = 491, 435, 407; calc. for [Mn(CO)$_3${MeC(CH$_2$^{80}SeMe)$_3$}]$^+$ *m*/*z* = 493, [Mn(CO){MeC(CH$_2$^{80}SeMe)$_3$}]$^+$ *m*/*z* = 437, [Mn{MeC(CH$_2$SeMe)$_3$}]$^+$ *m*/*z* = 409. ^{1}H NMR: δ 2.70 (*s*, 6 H, CH$_2$), 2.38 (*s*, 9 H, SeMe) and 1.27 (*s*, 3 H, CCH$_3$). ^{13}C-{^{1}H} NMR: δ 215.4–217.7 (CO), 40.8 (C), 38.9 (CH$_2$), 34.7 (SeCH$_3$) and 25.5 (C*C*H$_3$).

***fac*-[Mn(CO)$_3${MeC(CH$_2$TeMe)$_3$}]CF$_3$SO$_3$.** Yield 78%. Calc. for C$_{12}$H$_{18}$F$_3$MnO$_6$STe$_3$: C, 18.3; H, 2.3. Found: C, 18.9; H, 2.6%. Electrospray mass spectrum (MeCN): found *m*/*z* = 639, 583, 555; calc. for [Mn(CO)$_3${MeC(CH$_2$^{130}TeMe)$_3$}]$^+$ *m*/*z* = 643, [Mn(CO){MeC(CH$_2$^{130}TeMe)$_3$}]$^+$ *m*/*z* = 587, [Mn{MeC(CH$_2$TeMe)$_3$}]$^+$ *m*/*z* = 559. ^{1}H NMR: δ 3.00 (br, 6 H, CH$_2$), 2.06 (s, 9 H, TeCH$_3$) and 1.28 (*s*, 3 H, CCH$_3$). ^{13}C-{^{1}H} NMR: δ 216.5–222.1 (CO), 39.5 (C), 31.8 (CH$_2$), 29.0 (C*C*H$_3$) and −8.3 (TeCH$_3$).

***fac*-[Mn(CO)$_3${MeC(CH$_2$TePh)$_3$}]CF$_3$SO$_3$.** Yield 65%. Calc. for C$_{27}$H$_{24}$F$_3$MnO$_6$STe$_3$: C, 33.3; H, 2.5. Found: C, 34.3; H, 2.7%. Electrospray mass spectrum (MeCN): found *m*/*z* = 824; calc. for [Mn(CO)$_3${MeC(CH$_2$^{130}TePh)$_3$}]$^+$ *m*/*z* = 829. ^{1}H NMR: δ 7.4–7.7 (m, 15 H, Ph), 2.8–3.8 (br, 6 H, CH$_2$) and 1.2 (*s*, 3 H, CH$_3$). ^{13}C-{^{1}H} NMR: δ 215–220 (CO), 128–139 (Ph), 40.2 (C), 31.3 (CH$_3$) and 20.5 (CH$_2$).

***fac*-[Mn(CO)$_3${MeC(CH$_2$PPh$_2$)$_3$}]CF$_3$SO$_3$.** Yield 40%. Required for C$_{45}$H$_{39}$F$_3$MnO$_3$P$_3$S: C, 57.1, H, 4.1. Found: C, 57.6; H, 4.3%. Electrospray mass spectrum (MeCN): found *m*/*z* = 776, 763; calculated for [Mn(CO)$_3${MeC(CH$_2$PPh$_2$)$_3$}]$^+$ *m*/*z* = 763, [Mn(CO)$_2${MeC(CH$_2$PPh$_2$)$_3$}.MeCN]$^+$ *m*/*z* = 777. ^{1}H NMR: δ 6.9–7.7 (m, Ph, 30 H), 2.3–2.7 (m, CH$_2$, 6 H) and 1.1–1.3 (br, CH$_3$, 3 H). ^{13}C-{^{1}H} NMR: δ 212.8–221.9 (CO), 126.9–136.6 (Ph), 36.0 (C), 31.8 (CH$_2$ and 29.9 (CH$_3$).

[Mn(CO)$_3${Ph$_2$P(CH$_2$)$_2$PPh(CH$_2$)$_2$PPh$_2$}]CF$_3$SO$_3$. Yield 33%. Required for C$_{38}$H$_{33}$F$_3$MnO$_6$P$_3$S·CHCl$_3$: C, 49.7; H, 3.6. Found: C, 49.9; H, 3.9%. Electrospray mass spectrum (MeCN): found *m*/*z* = 674, 646, 617, 598; calculated for [Mn(CO)$_3${Ph$_2$P(CH$_2$)$_2$PPh(CH$_2$)$_2$PPh$_2$}]$^+$ *m*/z = 673, [Mn(CO)$_2${Ph$_2$P(CH$_2$)$_2$PPh(CH$_2$)$_2$PPh$_2$}]$^+$ *m*/*z* = 645, [Mn(CO){Ph$_2$P(CH$_2$)$_2$PPh(CH$_2$)$_2$PPh$_2$}]$^+$ *m*/*z* = 617, [Mn{Ph$_2$P(CH$_2$)$_2$PPh(CH$_2$)$_2$PPh$_2$}]$^+$ *m*/*z* = 599. ^{1}H NMR: δ 6.9–7.8 (m, Ph, 25 H) and 2.7–3.0 (m, CH$_2$, 8 H). ^{13}C-{^{1}H} NMR: 212.2–219.6 (CO), 39.0, 36.6 (CH$_2$).

***fac*-[Mn(CO)$_3$(PPh$_2$H)$_3$]CF$_3$SO$_3$.** Yield 58%. Required for C$_{40}$H$_{33}$F$_3$MnO$_6$P$_3$S: C, 56.7; H, 3.9. Found: C, 56.4; H, 4.2%. Electrospray mass spectrum (MeCN): found *m*/*z* = 697, 669, 511; calculated for [Mn(CO)$_3$(PPh$_2$H)$_3$]$^+$ *m*/z = 697, [Mn(CO)$_2$(PPh$_2$)$_3$]$^+$ *m*/*z* = 669, [Mn(CO)$_2$(PPh$_2$H)$_2$]$^+$ *m*/*z* = 511. ^{1}H NMR: 6.5–7.6 (m, Ph, 30 H) and 5.2–6.1 (m, PH, 3 H). ^{13}C-{^{1}H} NMR: δ 210.5–222.1 (br, CO) and 128.6–134.8 (Ph).

***fac*-[Mn(CO)$_3$(PCy$_2$H)$_3$]CF$_3$SO$_3$.** Yield 66%. Required for C$_{40}$H$_{69}$F$_3$MnO$_6$P$_3$S: C, 54.4; H, 7.8. Found: C, 54.7; H, 8.0%. Electrospray mass spectrum (MeCN): found *m*/*z* = 733, 535; calculated for [Mn(CO)$_3$(PCy$_2$H)$_3$]$^+$ *m*/*z* = 733, [Mn(CO)$_3$(PCy$_2$H)$_2$]$^+$ *m*/*z* = 535. ^{1}H NMR: δ 4.5 (m, PH, 3 H) and 1.1–2.2 (m, Cy, 66 H). ^{13}C-{^{1}H} NMR: δ 216.0–220.2 (br, CO) and 19.2–37.8 (Cy).

***fac*-[Mn(CO)$_3$(PPhH$_2$)$_3$]CF$_3$SO$_3$.** Yield 57%. Required for C$_{22}$H$_{21}$F$_3$MnO$_6$P$_3$S: C, 42.7; H, 3.4. Found: C, 42.2; H, 3.0%. Electrospray mass spectrum (MeCN): found *m*/*z* = 469, 441; calculated for [Mn(CO)$_3$(PPhH$_2$)$_3$]$^+$ *m*/z = 469, [Mn(CO)$_2$(PPhH$_2$)$_3$]$^+$ *m*/*z* = 441. ^{1}H NMR: δ 6.8–7.8 (m, Ph, 15 H) and 5.7 (m, PH, 6 H). ^{13}C-{^{1}H} NMR: δ 214.7–219.2 (br, CO) and 128.7–135.1 (Ph).

***fac*-[Mn(CO)$_3${MeC(CH$_2$AsMe$_2$)$_3$}]CF$_3$SO$_3$.** Yield 74%. Required for C$_{15}$H$_{27}$As$_3$F$_3$MnO$_6$S·CH$_2$Cl$_2$: C, 25.4; H, 3.8. Found: C, 25.2; H, 3.5%. Electrospray mass spectrum (MeCN): found *m*/*z* = 520; calculated for [Mn(CO)$_3${MeC(CH$_2$AsMe$_2$)$_3$}]$^+$ *m*/z = 523. ^{1}H NMR: δ 1.89 (*s*, CH$_2$, 6 H), 1.65 (*s*, AsMe, 18 H) and 1.02 (*s*, CCH$_3$, 3 H). ^{13}C-{^{1}H} NMR: δ 213–223 (br, CO), 49.2 (C), 37.8 (C*C*H$_3$), 33.5 (CH$_2$) and 15.3 (AsMe).

***fac*-[Re(CO)$_3${MeC(CH$_2$SeMe)$_3$}]CF$_3$SO$_3$.** Yield 26%. Required for C$_{12}$H$_{18}$F$_3$O$_6$ReSSe$_3$: C, 18.7; H, 2.3 Found: C, 19.2; H, 1.6%. Electrospray mass spectrum (MeCN): found *m*/*z* = 623; calculated for [^{185}Re(CO)$_3${MeC(CH$_2$^{80}SeMe)$_3$}]$^+$ *m*/z = 623. ^{1}H NMR (CD$_3$CN): δ 2.62 (*s*, SeMe, 9 H), 2.31 (*s*, CH$_2$, 6 H) and 1.33 (*s*, CCH$_3$). ^{13}C-{^{1}H} NMR: δ 187.5 (CO), 42.9 (C), 40.4 (CH$_2$), 34.9 (SeCH$_3$) and 31.0 (C*C*H$_3$).

X-Ray crystallographic studies

Details of the crystallographic data collection and refinement parameters are given in Table 9. Rigaku AFC7S four-circle diffractometer, *T* = 150 K (except for [Re(CO)$_3${MeC(CH$_2$SeMe)$_3$}]CF$_3$SO$_3$, 298 K), graphite monochromated Mo-Kα X-radiation (λ = 0.71073 Å). No significant crystal decay or movement was observed (except for [Mn(CO)$_3${MeC(CH$_2$PPh$_2$)$_3$}]CF$_3$SO$_3$·CH$_2$Cl$_2$, see below). The data were corrected for absorption using ψ-scans (except for [Mn(CO)$_3${MeS(CH$_2$)$_2$S(CH$_2$)$_2$SMe}]CF$_3$SO$_3$, see below). The structures were solved by heavy atom methods[23] and developed by iterative cycles of full-matrix least-squares refinement.[24]

[Mn(CO)$_3$([10]aneS$_3$)]$_2$[MnBr$_4$]. Small crystals of this compound were obtained by vapour diffusion of diethyl ether into a solution of [Mn(CO)$_3$([10]aneS$_3$)]Br in CH$_2$Cl$_2$. Some disorder was identified in the 6-membered chelate ring of one of the molecules. Attempts to model this did not reveal alternative positions for the atoms and there is one significant peak of unassigned electron density in this region (1.35 Å from S(5) and 1.50 Å from C(13)). The other cation, involving Mn(1), is well defined, as is the $MnBr_4^{2-}$ anion. The Mn, Br, S and O atoms were refined anisotropically and H atoms placed in fixed, calculated positions with *d*(C–H) = 0.96 Å.

[Mn(CO)$_3${MeS(CH$_2$)$_2$S(CH$_2$)$_2$SMe}]CF$_3$SO$_3$. The crystals were of rather poor quality and this restricted the data quality. ψ Scans did not give a satisfactory absorption correction and therefore the model was taken to isotropic convergence and DIFABS[25] was applied to the raw data. All non-H atoms were refined anisotropically and H atoms placed in fixed, calculated positions as above.

[Mn(CO)$_3${MeC(CH$_2$SMe)$_3$}]CF$_3$SO$_3$. All non-H atoms were refined anisotropically and H atoms were placed in fixed, calculated positions.

Table 9 Crystallographic data collection and refinement parameters

	$[Mn(CO)_3\{MeS(CH_2)_2S(CH_2)_2SMe\}]CF_3SO_3$	$[Mn(CO)_3([10]aneS_3)]_2[MnBr_4]$	$[Mn(CO)_3\{MeC(CH_2SeMe)_3\}]CF_3SO_3$	$[Mn(CO)_3\{MeC(CH_2PPh_2)_3\}]CF_3SO_3\cdot CH_2Cl_2$	$[Re(CO)_3\{MeC(CH_2SeMe)_3\}]CF_3SO_3$	$[Mn(CO)_3\{MeC(CH_2SMe)_3\}]CF_3SO_3$	$[Mn(CO)_3\{MeC(CH_2TePh)_3\}]CF_3SO_3$
Formula	$C_{10}H_{14}F_3MnO_6S_4$	$C_{20}H_{28}Br_4MnO_3S_6$	$C_{12}H_{18}F_3MnO_6SSe_3$	$C_{46}H_{41}Cl_2F_3MnO_6P_3S$	$C_{12}H_{18}F_3O_6ReSSe_3$	$C_{12}H_{18}F_3MnO_6S_4$	$C_{27}H_{24}F_3MnO_6STe_3$
M	470.39	993.23	639.14	997.65	770.41	498.44	971.28
Crystal system	Triclinic	Monoclinic	Triclinic	Monoclinic	Triclinic	Triclinic	Monoclinic
Space group	$P\bar{1}$	$P2_1/c$	$P\bar{1}$	$P2_1/n$	$P\bar{1}$	$P\bar{1}$	$P2_1/n$
a/Å	11.72(1)	7.430(5)	9.403(3)	10.948(2)	12.584(1)	9.190(1)	13.216(3)
b/Å	12.75(2)	28.273(3)	12.139(5)	22.611(3)	15.216(1)	12.085(2)	15.662(2)
c/Å	5.950(6)	6.075(5)	9.124(4)	18.429(3)	12.4563(8)	9.079(1)	16.050(4)
α/°	99.04(9)	—	100.15(3)	—	99.144(7)	98.85(1)	—
β/°	90.2(1)	95.79(4)	94.76(4)	97.99(1)	98.605(6)	94.78(1)	106.73(2)
γ/°	97.3(1)	—	80.92(3)	—	101.545(7)	81.450(10)	—
U/Å^3	871(1)	3359(2)	1010.5(7)	4517(1)	2266.2(3)	983.3(2)	3181(1)
Z	2	4	2	4	4	2	4
μ(Mo-Kα)/cm^{-1}	12.41	62.88	61.27	6.23	103.22	11.04	32.20
Unique observed reflections	3056	6056	3563	8174	7951	3469	5832
Observed reflections with $[I_o > 2\sigma(I_o)]$	2225	2629	2538	4161	4114	2732	2933
R	0.071	0.062	0.038	0.054	0.047	0.028	0.044
R'	0.099	0.068	0.042	0.065	0.055	0.026	0.046

$[Mn(CO)_3\{MeC(CH_2SeMe)_3\}]CF_3SO_3$. All non-H atoms were refined anisotropically and H atoms were placed in fixed, calculated positions.

$[Re(CO)_3\{MeC(CH_2SeMe)_3\}]CF_3SO_3$. Data were collected at 298 K and hence the thermal parameters are higher than for the other structures. The structure shows two independent cations and two anions in the asymmetric unit. Both CF_3SO_3 anions show some disorder. In one case the three F atoms are disordered through rotation about the C_3 axis. This was modelled successfully using alternative sites for each in a 50 : 50 ratio. In the other anion the O atoms are disordered *via* a rotation about the C–S bond, giving two alternative sites in a 70 : 30 ratio. The F atoms in this molecule also show some disorder, although attempts to refine these with split occupancies were unsuccessful, hence these were refined anisotropically with high thermal parameters. The Re, Se, S, C and the fully occupied F and O atoms were refined anisotropically and H atoms included in fixed, calculated positions.

$[Mn(CO)_3\{MeC(CH_2TePh)_3\}]CF_3SO_3$. All non-H atoms were refined anisotropically and H atoms placed in fixed, calculated positions.

$[Mn(CO)_3\{MeC(CH_2PPh_2)_3\}]CF_3SO_3\cdot CH_2Cl_2$. A linear decay correction was applied to take account of a 9% decay in the intensities of the standards during data collection. One CH_2Cl_2 solvent molecule was identified in the asymmetric unit. All non-H atoms were refined anisotropically and all of the H atoms associated with the phosphine ligand located in the difference map and included but not refined, while those associated with the CH_2Cl_2 solvent molecule were included in fixed, calculated positions.

CCDC reference number 186/1476.

See http://www.rsc.org/suppdata/dt/1999/2343/ for crystallographic files in .cif format.

Acknowledgements

We thank the EPSRC (J. C., S. D. O. and S. J. A. P.) and the University of Southampton for support.

References

1 E. G. Hope and W. Levason, *Coord. Chem. Rev.*, 1993, **122**, 109.
2 H. Schumann, A. A. Arif, A. L. Rheingold, C. Janiak, R. Hoffman and N. Kuhn, *Inorg. Chem.*, 1991, **30**, 1618 and refs. therein.
3 See P. M. Treichel, in *Comprehensive Organometallic Chemistry*, eds. E. W. Abel, F. G. A. Stone and G. Wilkinson, Pergamon, Oxford, 1982; *Comprehensive Organometallic Chemistry II*, eds. E. W. Abel, F. G. A. Stone and G. Wilkinson, Pergamon, Oxford, 1995.
4 J. Connolly, G. W. Goodban, G. Reid and A. M. Z. Slawin, *J. Chem. Soc., Dalton Trans.*, 1998, 2225; J. Connolly, M. K. Davies and G. Reid, *J. Chem. Soc., Dalton Trans.*, 1998, 3833; W. Levason, S. D. Orchard and G. Reid, *Organometallics*, 1999, **18**, 1275.
5 S. J. A. Pope and G. Reid, *J. Chem. Soc., Dalton Trans.*, 1999, 1615.
6 H. Elias, G. Schmidt, H.-J. Kuppers, M. Saher, K. Wieghardt, B. Nuber and J. Weiss, *Inorg. Chem.*, 1989, **28**, 3021.
7 W. Levason, S. D. Orchard and G. Reid, *J. Chem. Soc., Dalton Trans.*, 1999, 823.
8 J. Ellerman and H. A. Lindner, *Z. Naturforsch., Teil B*, 1976, **31**, 1350.
9 R. S. Nyholm, M. R. Snow and M. H. B. Stiddard, *J. Chem. Soc.*, 1965, 6534.
10 I. S. Butler, N. J. Coville and H. K Spendjian, *J. Organomet. Chem.*, 1972, **43**, 185.
11 R. Uson, V. Riera, J. Gimeno, M. Laguna and M. P. Gamasa, *J. Chem. Soc., Dalton Trans.*, 1979, 996.
12 G. A. Carriedo, V. Riera, M. L. Rodriguez and J. J. Sainz-Velicia, *Polyhedron*, 1987, **6**, 1879.
13 R. M. Nielson and S. Wherland, *Inorg. Chem.*, 1984, **23**, 3265.
14 D. Rehder, *Multinuclear NMR*, ed. J. Mason, Plenum, New York, 1987, ch. 19.
15 N. P. Luthra and J. D. Odom, in *The Chemistry of Organic Selenium and Tellurium Compounds*, eds. S. Patai and Z. Rappoport, Wiley, New York, 1986, vol. 1, ch. 6.
16 P. Garrou, *Chem. Rev.*, 1981, **81**, 229.
17 J. R. Bleeke and J. J. Kotyk, *Organometallics*, 1985, **4**, 194.
18 E. W. Abel, S. K. Bhargava, K. Kite, K. G. Orrell, V. Sik and B. L. Williams, *J. Chem. Soc., Dalton Trans.*, 1984, 365.
19 R. Ali, S. J. Higgins and W. Levason, *Inorg. Chim. Acta*, 1984, **84**, 65.
20 D. J. Gulliver, E. G. Hope, W. Levason, S. G. Murray, D. M. Potter and G. L. Marshall, *J. Chem. Soc., Perkin Trans. 2*, 1984, 429.
21 E. G. Hope, T. Kemmitt and W. Levason, *Organometallics*, 1987, **6**, 206; 1988, **7**, 78; T. Kemmitt and W. Levason, *Organometallics*, 1989, **8**, 1303.
22 R. G. Cunninghame, R. S. Nyholm and M. L. Tobe, *J. Chem. Soc.*, 1964, 580.
23 PATTY, The DIRDIF Program System, P. T. Beurskens, G. Admiraal, G. Beurskens, W. P. Bosman, S. Garcia-Granda, R. O. Gould, J. M. M. Smits and C. Smykalla, Technical Report of the Crystallography Laboratory, University of Nijmegen, 1992.
24 TEXSAN: Crystal Structure Analysis Package, Molecular Structure Corporation, The Woodlands, TX, 1995.
25 N. Walker and D. Stuart, *Acta Crystallogr., Sect. A*, 1983, **39**, 158.

Paper 9/02820J